Symmetric-group approach to the studies of spin-1/2 lattices

N. Flocke and J. Karwowski
Instytut Fizyki, Uniwersytet Mikołaja Kopernika, Grudziądzka 5, 87-100 Toruń, Poland
(Received 5 June 1996)

A technique for studying spin-1/2 lattices, based on the properties of the symmetric group $\mathcal{S}_N$, is presented. It is shown that the symmetric-group approach, applied to the Heisenberg Hamiltonian, leads to efficient diagonalization algorithms. Some examples of calculations for the lowest singlet and triplet states of the $2\times L$ isotropic antiferromagnetic Heisenberg ladders are compared with results in the literature. For the singlet-triplet gap we have obtained, by extrapolation to the bulk limit, the values 0.498 949 and 0.499 545 for a polynomial and an exponential fit, respectively. [S0163-1829(97)05310-1]

I. INTRODUCTION

Over the past few years a great amount of work has gone into analyzing the spectrum of the antiferromagnetic Heisenberg Hamiltonian describing interactions between spin particles. The motivation for this research comes from the important role antiferromagnetism seems to play when trying to explain the properties of high-T_c superconductors consisting of Cu oxide compounds, such as $Sr_{n-1}Cu_{n+1}O_{2n}$. It is believed that in these compounds two-dimensional CuO structures are responsible for superconductivity. Hence, most effort is now put into studies of the two-dimensional forms of the Heisenberg Hamiltonian.[1] In particular one is interested in the ground state of such systems and in the correlations between the different spins in the lattice. Another important question is whether an infinite lattice possesses a finite separation (gap) between its lowest-energy levels or not. These problems stimulated an enormous amount of work over the last dozen years, especially after Haldane's conjecture of a singlet-triplet gap for the infinite $S=1$ chain.[2]

Despite its simplicity, the exact treatment of the Heisenberg Hamiltonian is far from easy and very few results are known for infinite lattice systems. Probably the most famous result in this respect is the exact ground-state energy per spin for the infinite $S=1/2$ chain.[3] A corresponding result for higher-dimensional infinite spin-1/2 systems has so far been elusive. The most common approach in these cases is to perform exact calculations for a small number of finite systems and to extrapolate the results to the bulk limit. However, the number of spins in a lattice which can be treated exactly is severely limited by the combinatorial explosion of the dimension of the basis[4] and exact calculations for more than 24 spins without explicitly using symmetry properties of the lattice are next to impossible. In order to circumvent this problem, several approximation methods, like that of the resonating valence bond (RVB) method[5] or perturbational approaches[6], were designed, hoping to decrease effectively the dimensionality of the problem, without major losses in accuracy. The usual procedure for testing these approximate methods is to run them for a chain and to compare the obtained approximate result for the ground-state energy per spin with the known exact result. This offers some clues as to how good the approximations are and whether it is justified to extend them to higher-dimensional lattices.

Very recently a method, based on the early ideas of renormalization group techniques, has been developed and has become known as the density matrix renormalization group (DMRG) approach.[7] This method is based on the idea of successively building up the lattice from smaller sublattice units and works most accurately for open boundary conditions. As a consequence one is able to emulate the exact solutions for very large quasi-one-dimensional lattices and the DMRG algorithm is the source of the most accurate results for bulk limit properties of these systems so far.

The motivation for this paper is to examine, if one can exploit the well-known theory of the symmetric group $\mathcal{S}_N$ (Ref. 8) for exact diagonalization studies of spin-1/2 lattices. The power of methods utilizing properties of $\mathcal{S}_N$ in connection with spin-1/2 particles was recognized long ago in the context of performing calculations on the electronic structure of molecules, where the efficient evaluation of matrix elements of the Hamiltonian is crucial. The problem has been solved, within the so-called symmetric-group approach (SGA), for both spin-independent[9] and spin-dependent[10] Hamiltonians. A resulting computational method was successfully applied in molecular structure calculations.[11] The difference between the electronic molecular and the Heisenberg Hamiltonian is that the former operates in two kinds of spaces, namely, in the orbital and spin spaces, whereas the Heisenberg Hamiltonian is a pure spin operator and hence it operates in the spin space only. Hence, the Heisenberg Hamiltonian can be considered as an operator embedded in the molecular Hamiltonian and, in fact, it has been shown that the former can be obtained from the latter by neglecting contributions from the orbital space.[4,12] Therefore the SGA seems to be an appropriate tool for studying Heisenberg lattices. A further advantage of using the SGA in such calculations stems from the fact that one is able to perform them in the fully S,M-adapted subspaces rather than in the M-adapted ones. This considerably reduces the dimensions of the Hamiltonian matrices and in consequence one is able to treat larger lattices. Surprisingly, the use of the symmetric group to design algorithms for diagonalization of the Heisenberg Hamiltonian seems to be rather exceptional. In most of the works dealing with $\mathcal{S}_N$ theory in connection with the Heisenberg Hamiltonian, some fundamental and group-theoretical, rather than numerical, problems are addressed.[13,14] The aim of this paper is to demonstrate that

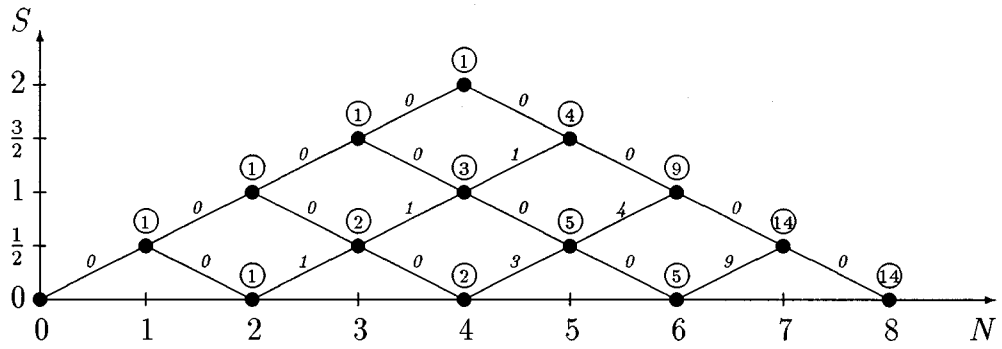

FIG. 1. Spin graph corresponding to a system of eight spins coupled to $S=0$.

$\mathcal{S}_N$ theory indeed allows us to write efficient codes for the exact treatment of spin-1/2 lattices. As an example, some calculations on the lowest singlet and triplet states of isotropic $2\times L$ antiferromagnetic Heisenberg ladders (AFHL's) are performed.

II. METHOD

The isotropic antiferromagnetic Heisenberg Hamiltonian for a system of N interacting spins is defined as[15]

$$\hat{H}=\sum_{\langle ij\rangle}^{N} J_{ij}\mathbf{S}_i\cdot\mathbf{S}_j, \tag{1}$$

where $\mathbf{S}_i$ denotes the spin operator of particle i, J_{ij} is the interaction constant with $J_{ij}>0$, and $\langle ij\rangle$ indicates that the sum runs over all interacting spin pairs. For a spin-1/2 system, the basis on which $\hat{H}$ operates consists of the set $\{\theta\}$ of all 2^N primitive spin product functions. This 2^N-dimensional basis can be symmetry adapted to the total spin S and to its projection M. The matrix representing $\hat{H}$ in this symmetry-adapted basis becomes block diagonal, each block being labeled by two quantum numbers S and M. In order to establish the connection between $\hat{H}$ and the symmetric group $\mathcal{S}_N$, we rewrite Eq. (1) in terms of permutations acting in the $\{\theta\}$ space, which can be easily done using the Dirac identity.[16] We obtain

$$\hat{H}=\frac{1}{2}\sum_{\langle ij\rangle}^{N} J_{ij}(ij)-\frac{1}{4}J, \tag{2}$$

where

$$J=\sum_{\langle ij\rangle}^{N} J_{ij} \tag{3}$$

and (ij) denotes a transposition interchanging spin i with j. Each of the above sets of S,M-adapted spin basis functions generates an irreducible representation of $\mathcal{S}_N$ labeled by a Young shape $[xy]$, in which x and y stand for the lengths of the upper and lower rows, respectively. The blocks of $\hat{H}$ corresponding to a given S value are associated with the irreducible representation (irrep) labeled by

$$x=\frac{N}{2}+S,\quad y=\frac{N}{2}-S, \tag{4}$$

and having dimension[17]

$$f^{xy}=\frac{x-y+1}{x+y+1}\binom{x+y+1}{y}. \tag{5}$$

Denoting the irreps of $\mathcal{S}_N$ by $\mathbf{\Gamma}^{[xy]}$, we can express the Hamiltonian matrix as

$$\mathbf{H}=\frac{1}{2}\sum_{\langle ij\rangle}^{N} J_{ij}\mathbf{\Gamma}^{[xy]}(ij)-\frac{1}{4}J\mathbf{I}, \tag{6}$$

where $\mathbf{I}$ stands for the unit matrix. From this equation we see that two major questions have to be considered: (1) how to handle the large $\mathcal{S}_N$-adapted spin space and (2) how to generate and deal with the representation matrices $\mathbf{\Gamma}^{[xy]}(ij)$ in an efficient way.

The first point can be solved in an elegant way using the concept of a spin graph.[18] The $\mathcal{S}_N$-adapted spin space is here represented in a very compact form using the branching diagram.[17] Each $\mathcal{S}_N$-adapted spin function is represented by a path in the spin graph, starting from the leftmost and ending at the rightmost vertex. An example of the spin graph is shown in Fig. 1.

To each vertex $V(N,S)$ there is associated a number indicating how many paths of the total spin S reach the coordinate (N,S), starting from $V(0,0)$, whereas the arcs $W(+,N,S)$ and $W(-,N,S)$, going up and down from the coordinate (N,S), respectively, are given the weights

$$W(+,N,S)=V(N,S+1), \tag{7}$$

$$W(-,N,S)=0, \tag{8}$$

with $V(N,S+1)=0$, if the vertex lies outside the graph. Hence each $\mathcal{S}_N$-adapted spin function can be uniquely indexed by a number $1\leqslant I\leqslant N$ obtained by summing over all arc weights of the corresponding path:

$$I=1+\sum_{i=1}^{N} W_i. \tag{9}$$

Each path can also be associated with a standard Young tableau in the following way: going up(+)/down(−) along the path corresponds to adding the next number in the upper/lower row of the corresponding Young shape. For example, in the spin graph shown in Fig. 1 we would make the following association:

$$++--+-+- \quad \Longrightarrow \quad \begin{array}{|c|c|c|c|}\hline 1 & 2 & 5 & 7 \\ \hline 3 & 4 & 6 & 8 \\ \hline \end{array} \tag{10}$$

From Eq. (9) we deduce that the index of this $\mathcal{S}_N$-adapted spin function is given by

$$I=1+0+0+0+0+3+0+9+0=13. \tag{11}$$

As we can see, the spin graph contains the whole information about the $\mathcal{S}_N$-adapted spin space. Even for very large N setting up the spin graph is trivial and requires negligible computer storage.

In order to set up an efficient algorithm for evaluation of $\mathbf{\Gamma}^{[xy]}(ij)$, we first note that each transposition can be written as a product of elementary transpositions, which exchange only consecutive labels. For example, if $i<j$ we have

$$(ij)=A(j-1\ j)A^{-1}, \tag{12}$$

where

$$A=\prod_{k=i+1}^{j-1}(k-1\ k). \tag{13}$$

Each $\mathbf{\Gamma}^{[xy]}(ij)$ can, therefore, be calculated by successive multiplications of the elementary $\mathbf{\Gamma}^{[xy]}(k-1\ k)$ ones, a process which obviously becomes prohibitive for large values of f^{xy}. But using iterative diagonalization methods like the one proposed by Davidson,[19] which is capable of extracting several lowest eigenvalues and eigenvectors at the same time (even in the presence of degeneracies), one never needs to construct the whole **H** matrix. Rather, only the evaluation of **HC** is required, where **C** is a vector of the same dimension as **H**. Looking at Eq. (6), one can see that an efficient algorithm for multiplying $\mathbf{\Gamma}^{[xy]}(k-1\ k)$ by **C** would solve the problem. Hence, the structure of the irrep matrices of these elementary transpositions should be as simple as possible. This is the case if one uses Young's orthogonal representation of $\mathcal{S}_N$,[8] in which the elementary $\mathbf{\Gamma}^{[xy]}(k-1\ k)$ is defined in terms of the action of $(k-1\ k)$ on the set of standard Young tableaux $\{T\}$ as follows:

$$\Gamma^{[xy]}(k-1\ k)_{ii}=-\frac{1}{d^i_{k-1,k}}=\rho_i, \tag{14}$$

$$\Gamma^{[xy]}(k-1\ k)_{ij}=\begin{cases}0 & \text{if } T_j=\text{nonstandard},\\ \sqrt{1-\rho_i^2} & \text{if } T_j=\text{standard}.\end{cases} \tag{15}$$

Here T_j is the tableau derived from T_i by interchanging numbers $k-1$ and k. The quantity $d^i_{k-1,k}$ is the so-called axial distance between numbers $k-1$ and k in tableau T_i and is defined as the number of steps to move from $k-1$ to k in the tableau, where moving right and up is counted as positive while moving left and down as negative. From the last two equations we deduce that

$$(k-1\ k)T_i=\rho_i T_i+\sqrt{1-\rho_i^2}T_j, \tag{16}$$

and from the association in Eq. (10) we can translate Eq. (16) into its spin-graphical form

(17)

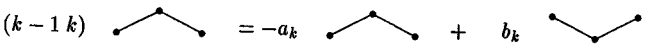

(18)

(19)

(20)

in which only the relevant path segments belonging to the transposition $(k-1\ k)$ are shown. The three vertices involved in these four kinds of segments are, from the left to the right, $V(k-2,S_{k-2})$, $V(k-1,S_{k-1})$, and $V(k,S_k)$, where S_{k-2}, S_{k-1}, and S_k are the corresponding coordinates on the S axis of the spin graph. The values of the two constants a_k and b_k in Eqs. (18) and (19) can be expressed in terms of the S_k coordinate:

$$a_k=\frac{1}{2S_k+1}, \quad b_k=\sqrt{1-a_k^2}. \tag{21}$$

The most important conclusion one can derive from Eqs. (17)–(20) is that they stand for a *whole set* of identical contributions to $\mathbf{\Gamma}^{[xy]}(k-1\ k)$ and that this matrix is composed of, at most, 1×1 and 2×2 submatrices along the diagonal. The multiplication $\mathbf{\Gamma}^{[xy]}(k-1\ k)\mathbf{C}$ can be performed in a very fast way, using the following algorithm.

(1) Loop over all left vertices V_l at the horizontal coordinate $k-2$ in the spin graph.

(2) For a given V_l, loop over the three possible right vertices V_r at the horizontal coordinate k.

(3) For a pair of vertices V_l and V_r, calculate a_k and b_k [Eq. (21)] and find the set of indices $\{I_h\}$ and $\{I_t\}$ [Eq. (9)] of all head and tail subpaths reaching V_l and leaving V_r, respectively.

(4) Loop over all pairs of I_h and I_t and add the contribution to $\mathbf{\Gamma}^{[xy]}(k-1\ k)\mathbf{C}$.

From Eqs. (12) and (13) we see that in order to construct a matrix corresponding to a transposition (ij), one has to perform $2|i-j|-1$ matrix multiplications. Hence, the numbering of the spin lattice should be done in such a way that the number of such multiplications is a minimum. To illustrate this point, let us consider the following ladder lattice, numbered in two different ways:

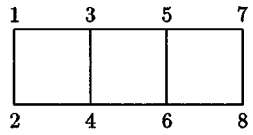

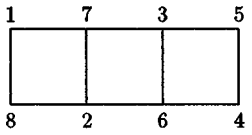

The first one requires 20 matrix multiplications, giving a very sparse **H** matrix, while for the second one 70 matrix

TABLE I. Ground-state ($S=0$) energies per spin in units of J of the *free* ϵ_0^f, *periodic* ϵ_0^p, and *Möbius* ϵ_0^m $2\times L$ AFHL lattices.

L	f^{xy}	ϵ_0^f	ϵ_0^p	ϵ_0^m
3	5	−0.521564206929	−0.508795939622	−0.625000000000
4	14	−0.536633307082	−0.602511171797	−0.548561218443
5	42	−0.544671206434	−0.563879285649	−0.589453358060
6	132	−0.550289372949	−0.584437168239	−0.570636012864
7	429	−0.554237575796	−0.573943000433	−0.581664843887
8	1430	−0.557216945222	−0.580203030314	−0.575676607240
9	4862	−0.559529675630	−0.576633142480	−0.579356425402
10	16796	−0.561381255868	−0.578859502513	−0.577182267851
11	58786	−0.562895857670	−0.577507129164	−0.578558041496
12	208012	−0.564158141975	−0.578372166804	−0.577704092845
13	742900	−0.565226206467	−0.577825861092	−0.578255595987
14	2674440	−0.566141701133	−0.578181575034	−0.577902373081

multiplications are needed and its **H** matrix is much more dense. Both **H** matrices are related by a similarity transformation generated by the orthogonal permutation matrix connecting both numbering schemes. Of course, both matrices have the same eigenvalues.

III. APPLICATION OF THE SGA METHOD TO $2\times L$ LADDERS

In order to test the algorithm, some calculations on the ground ($S=0$) and on the first excited ($S=1$) state have been performed for two-dimensional isotropic $2\times L$ AFHL lattices. Three types of boundary conditions have been chosen:

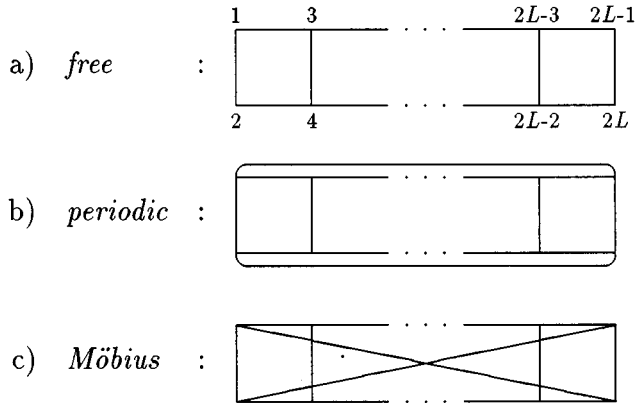

The node numbering is explicitly shown for the *free* ladder only. In the remaining cases the numbering is the same. Note that all *free* lattices of type (a) are nonfrustrated, whereas the *periodic* and *Möbius* ones are frustrated for L odd and even, respectively. The energy values per spin, ϵ_0, obtained for $S=0$ are presented in Table I to within 1×10^{-12} of accuracy.

The results obtained for ϵ_0^p, $L=4,6,8,10$, are in a complete agreement with those of Ref. 20. Only for $L=12$ is there a discrepancy in the last significant figure. The values for ϵ_0^f are strictly decreasing but they do not show any particularly good convergence rate to the bulk limit value ϵ_0^∞. The values for ϵ_0^p and ϵ_0^m, on the other hand, oscillate around ϵ_0^∞. An estimate of ϵ_0^∞ was obtained in Ref. 21 by taking the average of the two consecutive ϵ_0^p values for $L=11$ and $L=12$. A much better estimate can be obtained, if one takes the average values between ϵ_0^p and ϵ_0^m for each L. Three different ways of averaging were calculated, namely,

$$\overline{\epsilon^{p,m}}(L)=\{\epsilon_0^p(L)+\epsilon_0^m(L)\}/2, \tag{22}$$

$$\overline{\epsilon^{p,p}}(L)=\{\epsilon_0^p(L-1)+\epsilon_0^p(L)\}/2, \tag{23}$$

$$\overline{\epsilon^{m,m}}(L)=\{\epsilon_0^m(L-1)+\epsilon_0^m(L)\}/2. \tag{24}$$

The results are shown in Table II. From the first column of Table II, we can deduce that for the bulk limit $\epsilon_0^\infty\approx -0.578\,04$, if we assume $\epsilon_0^\infty=\overline{\epsilon^{p,m}}(\infty)$. To improve this result, we define the following quantities:

$$\Delta\overline{\epsilon}(L)=\overline{\epsilon^{p,m}}(L-1)-\overline{\epsilon^{p,m}}(L), \tag{25}$$

$$R(L)=\Delta\overline{\epsilon}(L-1)/\Delta\overline{\epsilon}(L). \tag{26}$$

Their values are shown in Table III. For any $L_i\leq L$ we have the exact relation

TABLE II. Results of different ways of averaging ϵ_0 values for the $2\times L$ AFHL lattices.

L	$\overline{\epsilon^{p,m}}$	$\overline{\epsilon^{p,p}}$	$\overline{\epsilon^{m,m}}$
3	−0.566897969811	-	-
4	−0.575536195120	−0.555653555710	−0.586780609222
5	−0.576666321855	−0.583195228723	−0.569007288252
6	−0.577536590552	−0.574158226944	−0.580044685462
7	−0.577803922160	−0.579190084336	−0.576150428376
8	−0.577939818777	−0.577073015374	−0.578670725564
9	−0.577994783941	−0.578418086397	−0.577516516321
10	−0.578020885182	−0.577746322497	−0.578269346627
11	−0.578032585330	−0.578183315839	−0.577870154674
12	−0.578038129825	−0.577939647984	−0.578131067171
13	−0.578040728540	−0.578099013948	−0.577979844416
14	−0.578041974058	−0.578003718063	−0.578078984534

TABLE III. Differences $\Delta\overline{\epsilon}$ between values of $\overline{\epsilon^{p,m}}$ and their ratios R.

L	$\Delta\overline{\epsilon}$	R
4	0.008638225309	-
5	0.001130126735	7.64359
6	0.000870268697	1.29860
7	0.000267331608	3.25539
8	0.000135896617	1.96717
9	0.000054965164	2.47241
10	0.000026101241	2.10584
11	0.000011700148	2.23085
12	0.000005544495	2.11023
13	0.000002598715	2.13355
14	0.000001245518	2.08645

$$\overline{\epsilon^{p,m}}(L)=\overline{\epsilon^{p,m}}(L_i)-\Delta\overline{\epsilon}(L_i)\sum_{k=1}^{L-L_i}\prod_{l=1}^{k}[R(L_i+l)]^{-1}, \tag{27}$$

from which we can derive for the bulk limit

$$\epsilon_0^{\infty}=\overline{\epsilon^{p,m}}(L_i)-\Delta\overline{\epsilon}(L_i)\sum_{k=1}^{\infty}\prod_{l=1}^{k}[R(L_i+l)]^{-1}. \tag{28}$$

If we knew all values of $R(L_i+l)$, $l=1,2,\ldots,\infty$, then we would be able to calculate ϵ_0^{∞} exactly. Defining a mean value $\overline{R}$ of all ratios, such that

$$\sum_{k=1}^{\infty}\prod_{l=1}^{k}[R(L_i+l)]^{-1}=\sum_{k=1}^{\infty}\frac{1}{\overline{R}^k}, \tag{29}$$

we get for $\overline{R}>1$

$$\epsilon_{0-}^{\infty}=\overline{\epsilon^{p,m}}(L_i)-\frac{\Delta\overline{\epsilon}(L_i)}{\overline{R}-1}. \tag{30}$$

Observing Table III we are led to the conjecture that $R(L)\to 2$ as $L\to\infty$; i.e., $R(L)$ stabilizes at the value of 2. Hence as a first approximation to $\overline{R}$ we can use the value of $R(14)$ and set $\overline{R}=\frac{1}{2}[R(14)+2]$. Using the values for $L_i=14$ we obtain from Eq. (30)

$$\epsilon_0^{\infty}\approx -0.578\,043\,168, \tag{31}$$

a value which compares very well with $-0.578\,043\,140$ obtained from a DMRG study.[22] The $R(L)$ stabilization comes as a surprise and it would be interesting to see if the same happens for more complex lattices for which a *periodic* and *Möbius* boundary condition can be defined (this would be the case for example for other $K\times L$ lattices, with $K>2$).

The results for the $S=1$ state of the $2\times L$ AFHL lattice are shown in Table IV. Also here we observe a rather poor convergence rate for the *free* boundary lattice, in contrast to the *periodic* and *Möbius* lattices. For the last two, the excited state energies per spin oscillate, but in contrast to the ground state they do not oscillate around the bulk limit value. Combining the results from Tables I and IV, we get for the singlet-triplet energy gaps

$$\Delta^f(L)=\{\epsilon_1^f(L)-\epsilon_0^f(L)\}\times 2L, \tag{32}$$

$$\Delta^p(L)=\{\epsilon_1^p(L)-\epsilon_0^p(L)\}\times 2L, \tag{33}$$

$$\Delta^m(L)=\{\epsilon_1^m(L)-\epsilon_0^m(L)\}\times 2L. \tag{34}$$

The corresponding numerical values are presented in Table V. The values for the *periodic* case agree again with those of Ref. 20 for $L=4,6,8,10$. A significant discrepancy (0.514 784 as compared to 0.514 999 in Ref. 20) appearing in the $L=12$ case is most likely due to a misprint in the table of this reference. To extrapolate the gaps to the bulk limit $\Delta(\infty)$, we took the values for $\Delta^p(L)$; $L=6,8,10,12$ and $\Delta^m(L)$; $L=5,7,9,11,13$ and applied a polynomial and an exponential fit of the forms

$$\Delta(L)=\Delta(\infty)+a_4L^{-4}+a_5L^{-5}+\cdots, \tag{35}$$

$$\Delta(L)=\Delta(\infty)+bL^{-c}e^{d/L}. \tag{36}$$

The fitting functions have been chosen to monotonically decrease as $1/L$ tends to zero and to have the derivative at this limit vanishing. The best fits have been obtained for the following values. (1) Polynomial: $\Delta(\infty)=0.498\,949$,

TABLE IV. Excited-state ($S=1$) energies per spin in units of J of the *free* ϵ_1^f, *periodic* ϵ_1^p, and *Möbius* ϵ_1^m $2\times L$ AFHL lattices.

L	f^{xy}	ϵ_1^f	ϵ_1^p	ϵ_1^m
3	9	−0.385032535440	−0.338462734401	−0.458333333333
4	28	−0.440357514339	−0.500000000000	−0.430448130733
5	90	−0.473309340025	−0.476266797694	−0.520377028315
6	297	−0.493625460612	−0.532223082044	−0.502294859393
7	1001	−0.507666799263	−0.518698080323	−0.539965516241
8	3432	−0.517778723700	−0.545365679519	−0.529713346398
9	11934	−0.525416412064	−0.537526886577	−0.549368572855
10	41990	−0.531363574244	−0.552454152895	−0.543293744759
11	149226	−0.536120612948	−0.547693912864	−0.554913296357
12	534888	−0.540006587350	−0.556922850527	−0.551142401294
13	1931540	−0.543238170205	−0.553906804883	−0.558599192957

TABLE V. Singlet-triplet energy gaps in units of J for the $2\times L$ AFHL lattices.

L	Δ^f	Δ^p	Δ^m
3	0.81919003	1.02199923	1.00000000
4	0.77020634	0.82008937	0.94490470
5	0.71361866	0.87612488	0.69076330
6	0.67996695	0.62656903	0.82009384
7	0.65199087	0.77342888	0.58379059
8	0.63101154	0.55739761	0.73541217
9	0.61403874	0.70391261	0.53978135
10	0.60035363	0.52810699	0.67777046
11	0.58905538	0.65589076	0.52018439
12	0.57963731	0.51478359	0.63748060
13	0.57168894	0.62189546	0.51106648

$a_4=568.923$, $a_5=-3309.4$, $a_6=5321.31$, and the rest of the coefficients zero. (2) Exponential: $\Delta(\infty)=0.499\,545$, $b=3838.38$, $c=4.577\,46$, and $d=-12.699$. The original points together with the points calculated by the fitting functions are collected in Table VI. In Fig. 2 we present a plot of the exponential fit. As we can see, both fits reproduce the original values with an accuracy of at least three significant figures. In both cases our extrapolated values for $\Delta(\infty)$ are slightly less than and very close to 0.5, which can be compared with $\Delta(\infty)=0.501$ from Ref. 20 obtained using exact diagonalization and Monte Carlo techniques under *periodic* boundary conditions and with $\Delta(\infty)=0.504$ from Ref. 22 obtained using the DMRG method under *free* boundary conditions. The discrepancy of 0.004 in the gap between our result and the result from Ref. 22 is probably due to different boundary conditions. However, more work on this subject is still needed. [Denoting by $\delta E_0(L)$ the absolute value of the difference between the ground-state energies of the nonfrustrated *free* and *closed* (*periodic* if L is even and *Möbius* if L is odd) lattices, we found a rapid exponential decay to $\delta E_0(\infty)\approx 0.3313$. Unfortunately, the corresponding $\delta E_1(L)$ values for the excited-state energies do not obey such a neat exponential decay. Therefore, the extrapolation to $\delta E_1(\infty)$ did not give a reliable result. The important point is, however, that if $\delta E_0(\infty)\neq\delta E_1(\infty)$, then the values for $\Delta(\infty)$ for the *free* and for the *closed* infinite $2\times L$ lattices differ. In other words, the effect of closing the *free* infinite lattice could result in an unequal shift of the two lowest-lying states.] Our results lead us to a conjecture that for the *periodic* isotropic $2\times\infty$ AFHL lattice it may be true that $\Delta(\infty)=1/2$.

IV. CONCLUSIONS

Using a method based on the theory of $\mathcal{S}_N$, we have performed ground-state ($S=0$) and excited-state ($S=1$) calculations for an isotropic $2\times L$ AFHL lattice for $L=3,4,\ldots,14$ and $L=3,4,\ldots,13$, respectively. Three different types of boundary conditions, i.e., *free*, *periodic*, and *Möbius*, have been imposed on these lattices. We have shown that one can obtain a very good estimate of the ground-state energy per spin by combining the results obtained for the *periodic* and *Möbius* lattices. The ground-state energies per spin for the *free* lattice do not show any good convergence rate to the bulk limit. Furthermore, our results suggest that for the *periodic* isotropic $2\times\infty$ AFHL lattice the singlet-triplet gap may have the exact value of 1/2.

The SGA procedure works very well in all the cases considered. Even very large eigenvalue problems, of dimensions up to more than 2.6×10^6, have been solved iteratively for the lowest eigenvalues. Our calculations were done using a Davidson routine which keeps all its vectors in the core memory. This severely limited accessible dimensions of **H**. Changing the diagonalization code, such that only two vectors are held at any time in the core memory, would allow for a treatment of matrices with dimensions up to 10^8 (corre-

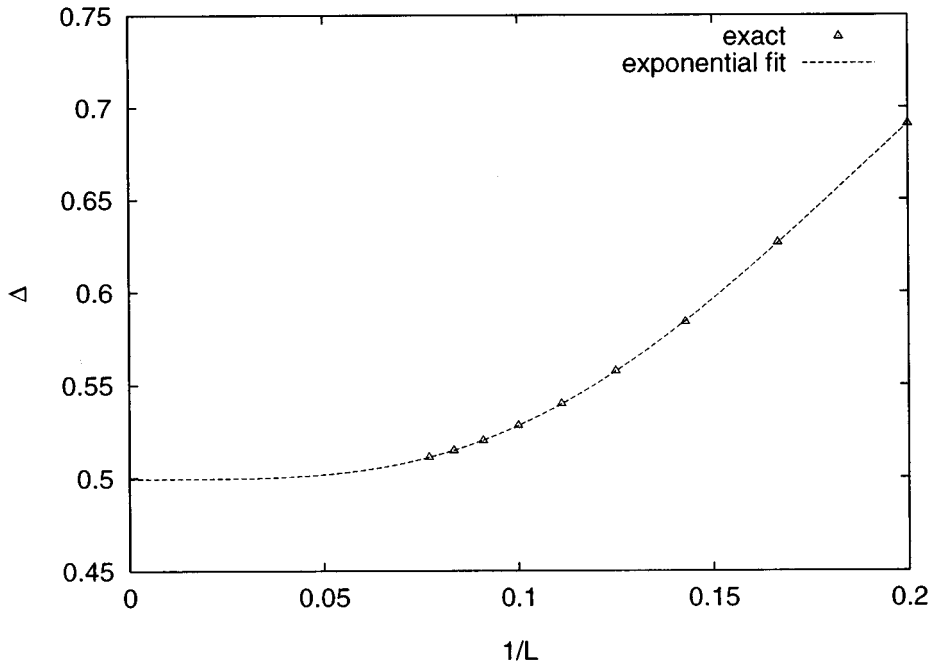

FIG. 2. Plot of Δ vs $1/L$ for the exact points and the exponential fit.

TABLE VI. Comparison of the original points with the points calculated by the polynomial and exponential fit.

L	Δ	Δ(poly)	Δ(exp)	Δ-Δ(poly)	Δ-Δ(exp)
5	0.69076330	0.69078193	0.69079974	−0.00001863	−0.00003644
6	0.62656903	0.62639636	0.62631084	0.00017267	0.00025819
7	0.58379059	0.58422602	0.58424131	−0.00043543	−0.00045072
8	0.55739761	0.55715095	0.55720749	0.00024666	0.00019012
9	0.53978135	0.53963015	0.53966319	0.00015120	0.00011816
10	0.52810699	0.52806904	0.52806618	0.00003795	0.00004081
11	0.52018439	0.52026254	0.52023824	−0.00007815	−0.00005385
12	0.51478359	0.51486807	0.51484274	−0.00008448	−0.00005915
13	0.51106648	0.51105825	0.51104931	0.00000832	0.00001717

sponding to $N=34$ for $S=0$). As far as the convergence rate of the diagonalization procedure is concerned, we found that generally the $S=1$ states required much more **HC** multiplications than the $S=0$ states. Further, the larger the dimension of **H**, the slower is the convergence.

The implicit S adaptation of the M-adapted spin space based on the SGA methodology leads to a substantial reduction of the dimension of the Heisenberg Hamiltonian matrix. However, one should keep in mind that the M-adapted spin space is more flexible, allowing also for the treatment of the XY and XYZ Hamiltonians, where the interaction between two spin sites cannot be written as a scalar product between the corresponding two spin operators. The S adaptation is of no use in these cases, since the Dirac identity cannot be applied. Hence, one pays simplicity and universality for lower dimensionality when going from the M-adapted spin space to the S,M-adapted one. One could even try to go further, introducing the lattice symmetry adaptation to the S,M-adapted spin space and thereby reducing the matrix dimensions even more.[23] Note that this problem can be formulated entirely within the $\mathcal{S}_N$ formalism, since the lattice point group G is isomorphic to a subgroup of $\mathcal{S}_N$. However, the complexity in writing such a lattice-symmetry-adapted program is formidable; moreover, it is still not clear how to generate the G,S,M-adapted lattice symmetry basis from the S,M-adapted basis in an efficient and direct way. The simple structure of the spin graph will become much more complicated and it is questionable if it is possible at all to represent the G,S,M-adapted basis in a graphical form. An application of projection-operator methods to establish the G,S,M-adapted bases, as advocated in Ref. 13, is very convenient for relatively small cases. However, when dimensions of the Hamiltonian matrices are very large, they become rather cumbersome, if not prohibitive.

ACKNOWLEDGMENTS

This work has been supported by the Polish KBN, Project No. 2 P03B 011 08. Helpful comments of Brian G. Wybourne are highly appreciated.

[1] For a review, see E. Dagotto and T.M. Rice, Science **271**, 618 (1996).
[2] F.D. Haldane, Phys. Lett. **93A**, 464 (1983).
[3] L. Hulthén, Ark. Mat. Astron. Fys. **26A**, 11 (1938).
[4] J. Karwowski, in *Symmetry and Structural Properties of Condensed Matter, Second International School of Theoretical Physics, Poznań, Poland*, edited by W. Florek, D. Lipiński, and T. Lulek (World Scientific, Singapore, 1992), p. 191.
[5] P.W. Anderson, Mater. Res. Bull. **8**, 153 (1973).
[6] T. Oguchi, H. Kitatani, and H. Nishimori, J. Phys. Soc. Jpn. **56**, 3858 (1987); R. F. Bishop, R. G. Hale, and Y. Xian, Int. J. Quantum Chem. **57**, 919 (1996).
[7] S.R. White, Phys. Rev. B **48**, 10 345 (1993).
[8] D.E. Rutherford, *Substitutional Analysis* (Edinburgh University Press, Edinburgh, 1948); G.D. James and A. Kerber, *The Representation Theory of the Symmetric Group* (Addison-Wesley, Reading, MA, 1981); B.E. Sagan, *The Symmetric Group* (Wadsworth & Brooks/Cole, Pacific Grove, CA, 1991).
[9] J. Karwowski, Theoret. Chim. Acta (Berlin) **29**, 151 (1973); W. Duch and J. Karwowski, Comput. Phys. Rep. **2**, 93 (1985).
[10] N. Flocke, M. Barysz, J. Karwowski, and G.H.F. Diercksen, Int. J. Quantum Chem. **61**, 1 (1997); **61**, 11 (1997); **61**, 21 (1997).
[11] G.H.F. Diercksen, W. Duch, and J. Karwowski, Chem. Phys. Lett. **168**, 69 (1990).
[12] D.J. Klein, W.A. Seitz, M.A. Garcia-Bach, J.M. Picone, and D.C. Foyt, Int. J. Quantum Chem. S. **17**, 555 (1983); S. Ramasesha and Z.G. Soos, Int. J. Quantum Chem. **25**, 1003 (1984).
[13] W.A. Seitz and D.J. Klein, Int. J. Quantum Chem. **7**, 647 (1973).
[14] P. Tavan, Z. Phys. B **72**, 277 (1988); Z. Yu and N. Lin, J. Phys. A **26**, L881 (1993).
[15] W. Heisenberg, Z. Phys. **49**, 619 (1928).
[16] P.A.M. Dirac, Proc. R. Soc. London, Ser. A **123**, 714 (1929).
[17] R. Pauncz, *Spin Eigenfunctions* (Plenum, New York, 1979).
[18] W. Duch, *GRMS or Graphical Representation of Model Spaces*, Lecture Notes in Chemistry Vol. 42 (Springer, Berlin, 1986).

[19] E.R. Davidson, J. Comput. Phys. **17**, 87 (1975); N. Kosugi, *ibid.* **55**, 426 (1984).
[20] T. Barnes, E. Dagotto, J. Riera, and E.S. Swanson, Phys. Rev. B **47**, 3196 (1993).
[21] E. Dagotto and A. Moreo, Phys. Rev. B **38**, 5087 (1988).
[22] S.R. White, R.M. Noack, and D.J. Scalapino, Phys. Rev. Lett. **73**, 886 (1994).
[23] W. Florek, D. Lipiński, and T. Lulek, in *Symmetry and Structural Properties of Condensed Matter, Second International School of Theoretical Physics, Poznań, Poland*, edited by W. Florek, D. Lipiński, and T. Lulek (World Scientific, Singapore, 1992), p. 389; P.N. Moustanis, A. Theophilou, and S. Thanos, in *Symmetry and Structural Properties of Condensed Matter, Third International School of Theoretical Physics, Zajączkowo, Poland*, edited by T. Lulek, W. Florek, and S. Wałcerz (World Scientific, Singapore, 1994), p. 97.